



# INTERNATIONAL JOURNAL OF CREATIVE RESEARCH THOUGHTS (IJCRT)

An International Open Access, Peer-reviewed, Refereed Journal

## EXTRACTION OF BLOOD VESSEL FROM FUNDUS IMAGES USING FRANGI FILTER AND MORPHOLOGICAL OPERATIONS

Anu Jemila. G. R,  
Research Scholar,

A. F. Julia Sterlin,  
ME Communication systems,

### I. INTRODUCTION

**Abstract:**-The human eye is the best organ that enables to see all around the environment. This eye may be compared to a camera in a sense that the image is created on the retinal of the eye; whereas in a traditional camera the image is formed on the film. The retinal is that the solely location where blood vessel can be directly captured. Retinal blood vessel is very important structures in retinal images. Automatic segmentation of the retinal blood vessel from retinal images would be a powerful and helpful tool for the medical diagnostics. So, the main purpose of the segmentation is to differentiate an object of the interest and the background from an image. This paper presents a general technique for segmenting out vascular structures in retinal images, and characterising the segmented blood vessels. Morphological preprocessing is used to emphasise linear structures such as vessels. Thresholding of the image is used to provide a segmented vascular mask. Frangi filters are used to enhance the blood vessel network prior to clustering. Most of the retinal blood vessel segmentation methodologies are evaluated on DRIVE and STARE databases. The proposed segmentation method is able to achieve comparable accuracy to other methods while being very close to the manual segmentation provided by the second observer in all datasets.

**keywords:** Retinal blood vessels, Morphological preprocessing, Thresholding, Frangi filters

Retinal blood vessels are a main anatomical structure that can be detectable in the retinal fundus image. The structure and feature variations reflect the impact of cardio vascular disease (CVD) such as cataract, diabetic retinopathy (DR), and hypertension, etc. The study and the analysis of retinal vessel geometric characteristics such as vessel diameter, branch angles, and branch lengths have become the basis of medical applications related to early diagnosis and effective monitoring of retinal pathology. Retinal image assessment by ophthalmologists is a vital step for identification of retinal pathology. A cataract is the most common cause of visual impairment in the industrialized world that accounts for more than half of visual deficiency. A cataract is a thick, overcast zone that structures in the lens of the eye. A cataract starts when proteins in the eye shape bunches that retain the lens from sending clear pictures to the retina. Early diagnosis and cure of the cataract can avoid serious effects including blindness. Recently, more artificial intelligence-based approaches such as supervised methods have become popular in this area. One of the fundamental steps in diagnosing diabetic retinopathy is the extraction of retinal blood vessels from fundus images. Although several segmentation methods have been proposed, this segmentation remains challenging due to variations in retinal vasculature network and image quality. Currently, the main challenges in retinal vessel segmentation are the noise and thin vessels. Vessel segmentation methods usually contain preprocessing steps aimed at enhancing the appearance of vessels.

In this section, a brief discussion of retinal vessel segmentation methods is given to provide some insight into different methods and is by an exhaustive review of this method. For segmenting the blood vessels the contour model using Extraction of Segment Profiles ESP algorithm [1] is used. Here, the closely parallel vessels or overlapped vessels cannot be segmented properly. Gabor wavelet [22] is used to detect the elongated blood vessels. In Gabor wavelet the transform is suitable for detecting edges and other singularities in the image. Deeply supervised and smoothly regularized network [14] has an advantage of end to end and pixel to pixel segmentation. Down sampling layers are removed by using automatic segmentation for retinal vessels by D-NET [17]. Here, low level information is difficult to remove. Retinal image enhancement was done by speeded up adaptive contrast enhancement (SUACE) [3]. It is used to enhance the superficial vein images that have been captured with infrared radiation in real time. It cannot be used to detect the components in retinal images such as fovea, optical disc and retinal lesions. Minimum spanning super-pixel [21] Tree detector can reserve the details inside the boundaries of the vessel. Also, it has low complexity. The accuracy of semantic segmentation is very less and the smoother boundary cannot be detected. Huo et al [9] has proposed the Elite multi-objective artificial bee colony segmentation algorithm (EMOABC). It is applied to extract the vessel from the background. Here, the extraction of blood vessel cannot be improved and the performance is abnormal. Kapur and otsu functions are used as the thresholding algorithms. In improved multi-scale line detection [30] the varying windows can measure the grey contrast between the considering pixel and the surrounding pixels in different scales and correct the responses of vessel pixels affected by the nearby darkest pixels. It can be increase the responses of background pixels having similar features with pale vessel pixels. The screening of confused pixel is not made.

Several diseases can be detected and diagnosed at a very early stage by observing changes in retinal blood vessel features. In basic line detector [15], instead of taking the original fundus image as an input for segmentation, inverted green channel image is considered as the input. In multi-scale line detector, instead of taking single line length of  $W$  pixels, varying lengths of lines are considered keeping window size constant to calculate the line responses. The drawbacks of the multi-scale line detector which are false vessel detection around the optical disc area and the noisy patches in the output. A new level set

formulation is proposed by using fuzzy region competition for selective image segmentation [12]. It is able to detect and track the arbitrary combination of selected objects or image components. This new formulation should be one of the first proposals in a framework of region competition for selective segmentation. Experiments on both synthetic and real images validate its advantages in selective level set segmentation. It is prone to confusing an object with its background due to local inhomogeneity.

A B-COSFIRE [11] filter achieves orientation selectivity by computing the weighted geometric mean of the output of a pool of Difference-of-Gaussians filters, whose supports are aligned in a collinear manner. It achieves rotation invariance efficiently by simple shifting operations. The proposed filter is versatile as its selectivity is determined from any given vessel-like prototype pattern in an automatic configuration process.

Qingyong Li, Min Zheng, Feng Li, [13] have propose a double-scale non-linear thresholding method based on vessel support regions. First, the double-scale filtering method is applied to enhance the contrast between the foreground vascular and the background stuffs. Second, they segment the fine and coarse vessels by the corresponding adaptive local thresholding and fixed-ratio thresholding method. Finally, they obtain the binary segmentation by fusion of fine and coarse vessels. This method achieves a fine segmentation in comparison with the other state-of-the-art unsupervised methods. An Automatic method [16] is proposed for segmenting the choroidal layer from macular images by using the level set framework. The 3D nonlinear anisotropic diffusion filter is used to remove all the OCT imaging artifacts including the speckle noise and to enhance the contrast. Choroidal thickness map and choroidal diseases are still not investigated. A convolutional neural network (CNNs) [7] is a composite of multiple elementary processing units, each featuring several weighted inputs and one output, performing convolution of input signals with weights and transforming the outcome with some form of nonlinearity. The performance of neural deep learning here and in generic vision tasks suggest that its full potential in medical imaging is yet to be revealed. The principal idea behind iterative vessel segmentation is that in a vessel enhanced image, the bright and large vessels overshadow the thinner fine vessel branches. In such a situation, global thresholding would extract only the large prominent vessels while the finer vessel branches would remain un-segmented. Thus, to include these fine vessels into the segmented vasculature estimate, iterative adaptive

global thresholding is used [17]. Redesigning the vessel segmentation on wide field images with greater than 200° FOV is required. The rest of the paper presents methodology, performance evaluation, results and discussion are explained below.

## II. METHODOLOGY

### A. Block Diagram Description

The retina is the sole location where blood vessels can be directly captured. Over the past decade, the research showed the retinal image has been widely used in the medical community for diagnosing and observing the progression of diseases. Thus, retinal blood vessels are very important structures in retinal images. Automatic segmentation of retinal blood vessels from retinal images would be a powerful and helpful tool for medical diagnostics. So, the main purpose of segmentation is to differentiate an object of interest from the background in an image. The block diagram for segmentation of retinal blood vessels from a retinal fundus image is shown in "Fig. 1"

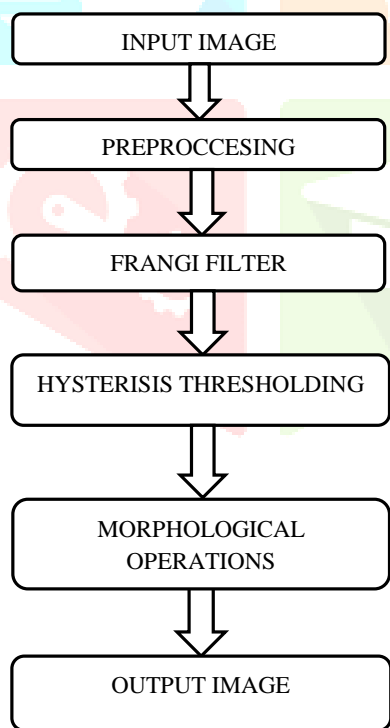


Fig.1 Block Diagram

### B. Preprocessing

The Fundus camera comprising of three channels of red, green and blue color, is used to capture the color fundus image. Among these three color channels, the red and blue channels do not have any contribution in the exalted information for the blood vessel detection and therefore, it is sufficient to exploit the green channel only. The green channel has the higher contrast between the vessels and the retinal background. The input retinal image is represented as a three layer image containing red, green and blue layers,

$$I = [I_R \quad I_G \quad I_B] \quad (3.1)$$

Where,  $I$  is the input RGB image.  $I_R, I_G, I_B$  represents the red, green and blue layers respectively. The green layer  $I_G$ , is chosen as it contains the signal of interest and therefore, used for blood vessels detection. The segmented RGB images are obtained by converting the labelled matrix to an RGB image. The random pixel elimination methodology is applied to merge small region to large neighbour pixels. Hence, the RGB colour model is a popular model that is widely used for display images in electronic systems such as computer and television. The RGB colour images are also used in photography. The segmentation of RGB images can have an impact on human's daily life problem such as examination of images generated within the medical field, analysis of images in forensic science etc. The color components are considered separately because green channel displays the best vessel/background contrast whereas the red and blue ones tend to be very noisy in case of RGB.

### C. Frangi Filter

Hessian matrix based Frangi filter is a popular approach that is both efficient and requires less computation time. The Hessian matrix is constructed by computing the vertical and horizontal diagonals of the images second order derivative. The Hessian-based vessel-ness filter can be defined as:

$$F(x) = \max_{\sigma} f(x, \sigma) \quad (3.2)$$

Where the pixel of interest is defined by  $x$ , the standard deviation for computing the Gaussian derivative of the image is denoted as  $\sigma$  and  $f$  represents the filter. The hessian matrix can be defined as:

$$H = \begin{pmatrix} H_{xx} & H_{xy} \\ H_{yx} & H_{yy} \end{pmatrix} \quad (3.3)$$

Where  $H_{xx}$ ,  $H_{xy}$ ,  $H_{yx}$  and  $H_{yy}$  represent the images directional second-order partial derivatives. Let's denote  $\lambda_1$  and  $\lambda_2$  as the eigenvalues of H where they are used for determining the probability of the pixel of interest  $x$  being a vessel based on the following notions:

$$|\lambda_1| \leq |\lambda_2| > 0 \text{ and } f(x, \sigma) = 0 \quad (3.4)$$

Then, the Hessian-based Frangi filter can be defined as:

$$f(x) = \begin{cases} 0, & \text{if } \lambda_2 > 0 \\ e^{\left(\frac{-R_b^2}{2a^2}\right)} \left(1 - e^{\left(\frac{S^2}{2\beta^2}\right)}\right), & \text{elsewhere} \end{cases} \quad (3.5)$$

$$R_b = \frac{|\lambda_1|}{|\lambda_2|}, S = \sqrt{\lambda_1^2 + \lambda_2^2} \quad (3.6)$$

where  $R_b$  and  $a$  are used for differentiating linear structures from blob like structures, while  $\beta$  and  $S$  are being used for differentiating background and vessels with the controlling parameters set ( $\alpha = 0.9, \beta = 13, \sigma = \{1, 1.1, 1.2, 1.3, \dots, 4\}$ ). The smoothing parameter  $\sigma$  was chosen to be varied from 1 to 4 in increments of 0.1 as it provided the best overall vessel enhancement. Selecting a small  $\sigma$  value will lose some thicker vessel details, whereas selecting a fixed large  $\sigma$  value will lose thinner vessel details. By varying the smoothing parameter  $\sigma$  and retaining the maximum pixel value from different scales, it is ensured that the vessels are enhanced and details are kept as much as possible.

#### D. Hysteresis Thresholding

An ordinary threshold transformation sets all pixels in the input image above a certain grey scale level to the value 1 and the remaining ones to the value 0. More generally, in mathematical terms, the threshold operator  $T$ , sets all pixels  $x$  of the input image  $f$  whose values lie in the range  $[t_i, t_j]$  to 1 and all others to 0,

$$\left[ T_{[t_i, t_j]}(f) \right] (x) = \begin{cases} 1, & \text{if } t_i \leq f(x) \leq t_j \\ 0, & \text{elsewhere} \end{cases} \quad (3.6)$$

Hysteresis thresholding uses two levels,  $t_{low}$  and a higher level  $t_{high}$ . Any pixel with grey-scale value above  $t_{high}$  is set to 1, as with ordinary thresholding. However, pixels that have a grey-scale value above  $t_{low}$  and are to pixels with grey-scale values above  $t_{high}$  are also set to 1. Isolated pixels above  $t_{low}$  are set to 0 (as are all pixels below  $t_{low}$ ). Thus, thin dark vessels above the  $t_{low}$  level that are connected to bright vessels above  $t_{high}$  are included in the vasculature mask. Hysteresis thresholding is easily implemented using morphological processing. Two binary images  $I_{low}$  and  $I_{high}$  are created;  $I_{low}$  by thresholding with the lower threshold value  $t_{low}$ , and  $I_{high}$  by thresholding with the higher threshold value  $t_{high}$ .  $I_{high}$  is then reconstructed into  $I_{low}$ . Mathematically,

$$HYST_{(t_{low}, t_{high})}(I) = R_{T_{[t_{low}, t_{max}]}}(I) \left[ T_{[t_{high}, t_{max}]}(I) \right], \quad (3.7)$$

Thus, the final mask image containing the vasculature  $I_m$ , can be created by hysteresis thresholding  $I_f$  with suitable values for  $t_{low}$  and  $t_{high}$ .

$$I_m = HYST_{(t_{low}, t_{high})}(I_f) \quad (3.8)$$

Typical values of threshold used range from 25 to 40 (on a scale of 0 to 255).

#### E. Morphological Operations

Morphology provides an attractive solution for detecting quasi-linear shapes such as vessels in an image. Since the vasculature is known to be piecewise linear, an algorithm that robustly extracts linear shapes is useful in vasculature extraction. The aim of the initial morphological filtering operation is to emphasize the vasculature, preserving vessel crossings and bifurcations. The approach used in this project uses the difference between the supremum and infimum of the openings of the original image  $I_0(x, y)$  with two linear structuring elements of different lengths.

Consider an image  $I_0(x, y)$  containing many bright linear shapes (the vessels) as well as flat homogeneous areas such as the background. A linear shape is defined as a bright part of an image with a minimum length  $L$  and a maximum width  $W$  (where usually  $W < L$ ). The vasculature in a retinal image is composed of many such connected linear shapes, and the aim of our initial processing is to preserve image

structures which satisfy the criteria of being at least  $L$  pixels long, and no more than  $W$  pixels wide. Morphological opening with a structuring element of a given shape preserves image structures that can contain the structuring element and removes those that cannot. Thus, opening the image with a linear structuring element  $B$ , of length  $L_1$  and width 1 preserves linear shapes when the structuring element and the shape are approximately parallel. If many such structuring elements are used, with different angular rotations, then all linear shapes with length greater than or equal to  $L_1$  should be preserved by at least one rotation. Noise and other non-vessel structures that cannot contain the structuring element at any rotation will not be preserved by such an operation. Thus, a cleaner version  $I_c$  of the image  $I_o$ , can be obtained by taking the supremum of the openings of the image with linear structuring elements with many different rotations. Mathematically this can be expressed as:

$$I_c = \sup_{i=1, \dots, 12} \{\gamma_{B_i}(I_o)\} \quad (3.9)$$

Where  $B_i$  represents structuring element  $B$  at rotation  $i$ , and twelve rotations of the single pixel structuring elements each  $15^\circ$  apart are used. In our particular case, the value of  $L_1$  used was 17 pixels. The length of the structuring element should be chosen so as to preserve vessels but remove noise and non-vessel structures. While the length of the optimal structuring element for a given retinal image depends on the tortuosity of the vessels in the image and the amount of noise present, the overall algorithm is relatively insensitive to small changes in the value of  $L_1$ .

Morphological re-construction extracts the peaks in a mask (conditioning) image that are touched by a marker image. If the image produced by “(3.9)” is used as the marker image and the original image is used as the mask image then an improved version of “(3.9)”, incorporating reconstruction, is

$$I_c = R_{I_o}(\sup_{i=1, \dots, 12} \{\gamma_{B_i}(I_o)\}) \quad (3.10)$$

This operation provides a significantly cleaner version of the image but is not sufficient to allow final segmentation of the vasculature. The operation of “(3.10)” preserves large homogeneous regions whose size exceeds  $L_1$  pixels in at least one dimension, and is thus of little use alone. This is because such regions can clearly contain the structuring element, (in at least one direction) and are thus preserved by “(3.10)”. A method is required that preserves only linear shapes which do not exceed a desired width.

Opening the image with a single-pixel linear structuring element,  $B$ , of length  $L_1$ , preserves linear shapes. A corollary to this is that opening the image with a linear structuring element,  $B$ , of length  $L_2$  and width 1 removes linear shapes when the structuring element and the shape are approximately orthogonal. Removing the linear shapes from an image corresponds to replacing them by their (local) background. Thus for a linear shape of width less than  $L_2$  there is at least one direction in which opening with a linear structuring element  $B$  of length  $L_2$  will remove the shape. Thus, the local background image can be obtained by taking the infimum of openings with a linear structuring element  $B$  of length  $L_2$  taken in many directions. Mathematically,

$$I_B = \inf_{i=1, \dots, 12} \{\gamma_{B_i}(I_o)\} \quad (3.11)$$

where, twelve structuring elements at angles from  $0^\circ$  to  $165^\circ$  are used. The value of  $L_2$  used in our processing is 17 pixels. This operation preserves large homogenous areas of colour but also removes small linear shapes. There are now two images;  $I_c$ , that contains both the linear shapes and the large homogenous areas and another image,  $I_B$  which contains only the large homogenous areas. Subtracting these images will yield a third image,  $I_V$ , which contains only the linear shapes.

$$I_V = I_c - I_B \quad (3.12)$$

To summarize, this initial morphological filtering stage yields an image  $I_V$  that contains only linear shapes.

### III. PERFORMANCE EVALUATION

True positive (TP) denotes vessel pixels correctly segmented as vessel pixels while true negative (TN) denotes non-vessel pixels correctly segmented as non-vessel pixels. False positive (FP) denotes non-vessel pixels segmented as vessel pixels, while false negative (FN) denotes vessel pixels segmented as non-vessel pixels.

Accuracy represents the overall performance of a segmentation method and is computed by:

$$\begin{aligned} \text{Accuracy} &= \frac{\text{total TP} + \text{total TN}}{\text{total TP} + \text{total TN} + \text{total FP} + \text{total FN}} \end{aligned}$$

The precision rate was computed by the following formula;

$$\text{Precision} = \frac{\text{total TP}}{\text{total TP} + \text{total FP}}$$

#### IV. RESULTS AND DISCUSSION

##### A. Databases

Most of the retinal blood vessel segmentation methodologies are evaluated on DRIVE and STARE databases. The name of the DRIVE database has well expressed its purpose to enable comparative studies on segmentation of blood vessel in the retinal image. The DRIVE database consists of the 40 colour retinal image, the 40 images are randomly selected from 400 diabetic subjects between 25-90 years of age, and 33 do not show any sign of diabetic retinopathy whereas 7 show signs of mild early diabetic retinopathy.

The STARE database contains 400 retinal colour images. The images have been acquired using a Topcon TRV-50 fundus camera with a 35-degree field of view. Each image has been captured using 8 bits per colour plane at 605 by 700 pixels, and the approximate diameter of the field of view is 650 by 500. The 20 of the images can be utilized for blood vessel segmentation because they are with the vessel ground truth images. The sample input image is shown in "Fig.2"



Fig.2. Input Image

##### B. Preprocessing

The Fundus camera comprising of three channels of red, green and blue color, is used to capture the color fundus image. Among these three color channels, the red and blue channels do not have any contribution in the exalted information for the blood vessel detection and therefore, it is sufficient to exploit the green channel only. The green channel has the higher contrast between the vessels and the retinal background. The proposed method works on the

inverted green channel images, where vessels appear brighter than the background. The output of preprocessing stage is shown in "Fig. 3".

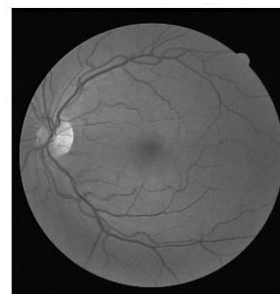


Fig.3. Green channel Image

##### C. Image Enhancement

Frangi filter is used in coronary segmentation by enhancing the vessel profiles. Image enhancement is to improve the interpretability or perception of information in images for human viewers. Hessian matrix based Frangi filter is a popular approach that is both efficient and requires less computation time. The Hessian matrix is constructed by computing the vertical and horizontal diagonals of the images second order derivative. The smoothing parameter  $\sigma$  was chosen to be varied from 1 to 4 in increments of 0.1 as it provided the best overall vessel enhancement. Selecting a small  $\sigma$  value will lose some thicker vessel details, whereas selecting a fixed large  $\sigma$  value will lose thinner vessel details. By varying the smoothing parameter  $\sigma$  and retaining the maximum pixel value from different scales, it is ensured that the vessels are enhanced and details are kept as much as possible. The enhanced image is shown in "Fig. 4".

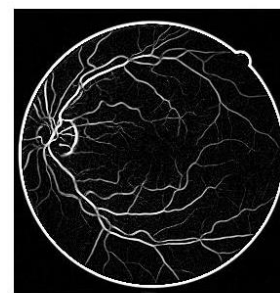


Fig.4. Output of Frangi Filter

##### D. Morphological Operations

Morphology provides an attractive solution for detecting quasi-linear shapes such as vessels in an image. Since the vasculature is known to be piecewise linear, an algorithm that robustly extracts linear shapes is useful in vasculature extraction. The aim of the

initial morphological filtering operation is to emphasize the vasculature, preserving vessel crossings and bifurcations. The approach used in this project uses the difference between the supremum and infimum of the openings of the original image with two linear structuring elements of different lengths. To summarize, this initial morphological filtering stage yields an image  $I_V$  that contains only linear shapes. The output image is shown in “Fig.5”.

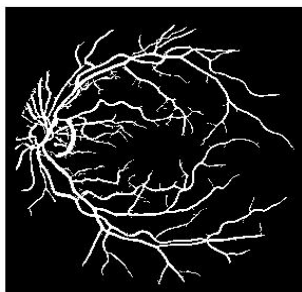


Fig.5. Vessel Segmentation

The findings and their values are summarized in the Table. I

Parameters	Values
1. Accuracy	0.96052
2. Precision	0.75637

Table I. accuracy and precision values

## V. CONCLUSION AND FUTURE WORK

The quality of the segmentation is dependent on a number of parameters such as image quality, choice of threshold, and choice of structuring elements. Successful segmentation allows a variety of further processing such as: Visual highlighting of vessels in the image, accurate characterization of vessel parameters such as thickness and tortuosity and Location of vessel bifurcation and crossings which can act as intrinsic features for registration schemes. In this study, a retinal vessel segmentation algorithm based on morphological operations and hysteresis thresholding was proposed. Utilizing morphological processes and filtering techniques, the images were enhanced. For a typical image, it is reasonable to expect that approximately 90% of vessels will be detected, and that approximately 10% of non-vessel pixels will be incorrectly classified as vessels. In

advanced retinal image analysis, the segmented vasculature tree can be used to calculate the vessel diameter and tortuosity, discriminating veins and arteries along with measuring the arteriovenous ratio. Finally, the vessels were segmented by morphological operations. The proposed method was able to handle noisy and pathological images and produce good segmentation, especially in thinner vessels while being computationally efficient.

Future efforts can be directed towards the implementation of such modified proposed architectures for the detection of tiny branched blood vessel, pigment epithelial detachments and other macular degenerative pathologies.

## VI.

### VII. REFERENCES

- [1] Al-Diri, B., Hunter, A., & Steel, D. (2009). “An Active Contour Model for Segmenting and Measuring Retinal Vessels”. *IEEE Transactions on Medical Imaging*, 28(9), 1488–1497.
- [2] Azzopardi, G., Strisciuglio, N., Vento, M., & Petkov, N. (2015). “Trainable COSFIRE filters for vessel delineation with application to retinal images”. *Medical Image Analysis*, 19(1), 46–57.
- [3] Bandara, A. M. R. R., & Giragama, P. W. G. R. M. P. B. (2017). “A retinal image enhancement technique for blood vessel segmentation algorithm”. *2017 IEEE International Conference on Industrial and Information Systems (ICIIS)*.
- [4] Bashir Al-Diri, Andrew Hunter, David Steel, Maged Habib, TaghreedHudaib, and Simon Berry. (2008) “Review - a reference data set for retinal vessel proles”. *IEEE Engineering in Medicine and Biology Society*, pages 2262-2265.
- [5] Biswal, B., Pooja, T., & Bala Subrahmanyam, N. (2018). “Robust retinal blood vessel segmentation using line detectors with multiple masks”. *IET Image Processing*, 12(3), 389–399.
- [6] Etienne Decencire, Xiwei Zhang, Guy Cazuguel, Bruno Lay, BatriceCochener, and Jean-Claude Klein. (2014) “Feedback on a publicly distributed database”: the messidor

- database. *Image Analysis & Stereology*, 33(3):231-234.
- [7] Jiang, Y., Tan, N., Peng, T., & Zhang, H. (2019). "Retinal Vessels Segmentation Based on Dilated Multi-Scale Convolutional Neural Network". *IEEE Access*, 1–1.
- [8] Joes Staal, Michael D. Abramo, Mein dert Niemeijer, Max A. Viergever, and Bram van Ginneken.(2005) "Ridge based vessel segmentation in color images of the retina". *IEEE Transactions on Medical Imaging*, 23(4):501-509.
- [9] khomri, B., Argyrios, C., Djerou, L., Babahenini, M. C., & Cheriet, F. (2018). "Retinal blood vessel segmentation using the elite-guided multi-objective artificial bee colony algorithm". *IET Image Processing*.
- [10] Kirbas, C.; Quek, (2004) "A review of vessel extraction techniques and algorithms". *ACM Comput. Surv. CSUR 2004*, 36, 81–121.
- [11] Kolb, H. *Simple Anatomy of the Retina*, (2012). "Simple Anatomy of the Retina By Helga Kolb". *IET Image Processing*.
- [12] Li, B. N., Qin, J., Wang, R., Wang, M., & Li, X. (2016). "Selective Level Set Segmentation Using Fuzzy Region Competition". *IEEE Access*, 4, 4777–4788.
- [13] Li, Q. (2019). "Retinal Image Segmentation Using Double-Scale Nonlinear Thresholding on Vessel Support Regions". *CAAI Transactions on Intelligence Technology*.
- [14] Lin, Y., Zhang, H., & Hu, G. (2018). "Automatic Retinal Vessel Segmentation via Deeply Supervised and Smoothly Regularized Network". *IEEE Access*, 1–1.
- [15] Liskowski, P., & Krawiec, K. (2016). "Segmenting Retinal Blood Vessels with Deep Neural Networks". *IEEE Transactions on Medical Imaging*, 35(11), 2369–2380.
- [16] Marín, D., Aquino, A., Gegundez-Arias, M. E., & Bravo, J. M. (2011). "A New Supervised Method for Blood Vessel Segmentation in Retinal Images by Using Gray-Level and Moment Invariants-Based Features". *IEEE Transactions on Medical Imaging*, 30(1), 146–158.
- [17] MeindertNiemeijer, Mathieu Lamard, Chisako Muramatsu, Xiangqian Wu, and Michael D Abramo.(2010) Retinopathy online challenge: "Automatic detection of microaneurysms in digital color fundus photographs". *IEEE Transactions on Medical Imaging*, 29(1):185-195.
- [18] R. C. Gonzalez and R. E. Woods, (2002) "digital image processing", Pearson education.
- [19] Roychowdhury, S., Koozekanani, D. D., & Parhi, K. K. (2015). "Iterative Vessel Segmentation of Fundus Images". *IEEE Transactions on Biomedical Engineering*, 62(7), 1738–1749.
- [20] Shah, S. A. A., Shahzad, A., Khan, A., Lu, C.-K., & Tang, T. B. (2019). "Unsupervised Method for Retinal Vessel Segmentation based on Gabor Wavelet and Multi-scale Line Detector". *IEEE Access*, 1–1.
- [21] Sheng, B., Li, P., Mo, S., Li, H., Hou, X., Wu, Q., Feng, D. D. (2018). "Retinal Vessel Segmentation Using Minimum Spanning Super-pixel Tree Detector". *IEEE Transactions on Cybernetics*, 1–13. doi:10.1109/tyb.2018.2833963
- [22] Soares, J. V. B., Leandro, J. J. G., Cesar, R. M., Jelinek, H. F., & Cree, M. J. (2006). "Retinal vessel segmentation using the 2-D Gabor wavelet and supervised classification". *IEEE Transactions on Medical Imaging*, 25(9), 1214–1222.
- [23] Soomro, T. A., Mahmood Khan, T., Khan, M. A. U., Gao, J., Paul, M., & Zheng, L. (2018). "Impact of ICA-Based Image Enhancement Technique on Retinal Blood Vessels Segmentation". *IEEE Access*, 6, 3524–3538.
- [24] Sorri Iris Raninen Asta Voutilainen Raija Kamarainen Joni Lensu Lasse Kauppi Tomi, Kalesnykiene Valentina and Uusitalo Hannu. Diaretdb1 v2.1 – (2009) "diabetic retinopathy database and evaluation protocol".
- [25] The stare project structured analysis of the retina, (2005). "Structured Analysis of the Retina", *IEEE Transactions on Medical Imaging*, 23(4):501-509.
- [26] Thomas Kohler, Attila Budai, Martin F. Kraus, Jan Odstrcilik, Georg Michelson, and Joachim Hornegger.(2013) "Automatic no-reference quality assessment for retinal fundus images using vessel segmentation". In *Proceedings of the 26th IEEE International Symposium on Computer-Based Medical Systems*, pages 95-100.



- [27] Wang, C., Wang, Y. X., & Li, Y. (2017). Automatic Choroidal Layer Segmentation Using Markov Random Field and Level Set Method. *IEEE Journal of Biomedical and Health Informatics*, 21(6), 1694–1702.
- [28] Wang, W., wang, weihua, & Hu, Z. (2019). “A Retinal Vessel Segmentation Approach based on Corrected Morphological Transformation and Fractal Dimension”. *IET Image Processing*.
- [29] Yue, K., Zou, B., Chen, Z., & Liu, Q. (2018). “Improved multi-scale line detection method for retinal blood vessel segmentation”. *IET Image Processing*, 12(8), 1450–1457.
- [30] Zhang, J., Cui, Y., Jiang, W., & Wang, L. (2015). “Blood Vessel Segmentation of Retinal Images Based on Neural Network”. *Image and Graphics*, 11–17.

